Geophysical Research Letters

RESEARCH LETTER
10.1029/2019GL084886

Assessment of ICESat-2 Ice Sheet Surface Heights, Based on Comparisons Over the Interior of the Antarctic Ice Sheet

K. M. Brunt[1,2], T. A. Neumann[2], and B. E. Smith[3]

[1]Earth System Science Interdisciplinary Center, University of Maryland, College Park, MD, USA, [2]NASA Goddard Space Flight Center, Greenbelt, MD, USA, [3]Applied Physics Laboratory, University of Washington, Seattle, WA, USA

Key Points:
- We compare ground-based and satellite-derived height data
- The ground-based methods are internally consistent and accurate, with a precision of 5.6 cm
- NASA's latest satellite laser altimeter has <5 cm height accuracy and <13 cm surface measurement precision

Correspondence to:
K. M. Brunt,
kelly.m.brunt@nasa.gov

Citation:
Brunt, K. M., Neumann, T. A., & Smith, B. E. (2019). Assessment of ICESat-2 ice sheet surface heights, based on comparisons over the interior of the Antarctic ice sheet. *Geophysical Research Letters*, *46*, 13,072–13,078. https://doi.org/10.1029/2019GL084886

Received 13 AUG 2019
Accepted 23 OCT 2019
Published online 16 NOV 2019

Abstract We collected kinematic Global Navigation Satellite Systems (GNSS) surface height data, on a 750-km ground-based traverse of the flat interior of the Antarctic ice sheet, for comparison with Ice, Cloud, and Land Elevation Satellite-2 (ICESat-2) surface heights. Vertical errors in the GNSS data are estimated to be 5.6 cm, comparable to results from a previous traverse and with year-to-year comparisons. Comparisons of the GNSS heights and 6 months of ICESat-2 ATL03 photon-based heights and ATL06 segment-based heights indicate that the accuracy and precision of ICESat-2 data are comparable to that of results from the ICESat mission: ATL03 is currently accurate to better than 5 cm with better than 13 cm of surface measurement precision, while ATL06 is currently accurate to better than 3 cm with better than 9 cm of surface measurement precision.

Plain Language Summary NASA launched a satellite laser altimeter in 2018 with a mission that includes the determination of the surface height of our ice sheets with centimeter-level accuracy. This level of accuracy is required because centimeter-level changes in height over the vast Antarctic ice sheet constitute substantial changes in mean sea level rise. To validate that the new satellite is meeting those goals, NASA conducted a ground-based traverse to collect highly accurate and highly precise Global Navigation Satellite Systems surface height data for direct comparison with the satellite-derived surface heights. Our results show that the ground-based data are ideal for this type of validation and that the satellite data are meeting the early-mission accuracy and precision expectations.

1. Introduction

The National Aeronautics and Space Administration (NASA) Ice, Cloud, and Land Elevation Satellite-2 (ICESat-2) launched 15 September 2018, with mission goals that include determining centimeter-scale changes in ice sheet surface height to quantify their contributions to sea level rise (Markus et al., 2017). The single instrument on board ICESat-2, the Advanced Topographic Laser Altimeter System (ATLAS), is a photon-counting laser altimeter using 532 nm wavelength laser pulses (Neumann et al., 2018, 2019).

ATLAS has a single laser source, which is split into six beams to create six "spots" on the ground. Each ATLAS pulse contains trillions of photons; up to 10 of these photons return to the instrument, where their arrival time is recorded using single-photon sensitive detectors. The spatial profile of the ATLAS footprint is within 10% of a Gaussian distribution with a diameter of ~17 m. Given the random sampling of photons from the transmitted laser pulse, the received photons, when combined with knowledge of the ATLAS pointing direction and position in space, yield individual height measurements that are Gaussian-distributed across the illuminated area.

ATLAS not only detects photons reflected from the Earth's surface (signal) but also photons from ambient sunlight whose wavelengths fall within a narrow band (±0.015 nm) around the laser wavelength (solar background). A low-level ICESat-2 data product algorithm geolocates individual photons (Neumann et al., 2019) and passes this information to higher-level data product algorithms (e.g., Smith et al., 2019) that are unique to geophysical surface type, such as land ice, sea ice, and ocean.

The six individual ATLAS beams are arranged in three pairs with three relatively strong beams and three relatively weak beams (Neumann et al., 2019). Thus, the ATLAS "reference ground track" (RGT) is a single imaginary centerline of the ground track pattern. Within each beam pair the resultant spots are separated by 90 m across track to provide instantaneous knowledge of local slope. The three pairs of spots are separated by

©2019. American Geophysical Union. All Rights Reserved.
This is an open access article under the terms of the Creative Commons Attribution License, which permits use, distribution and reproduction in any medium, provided the original work is properly cited.

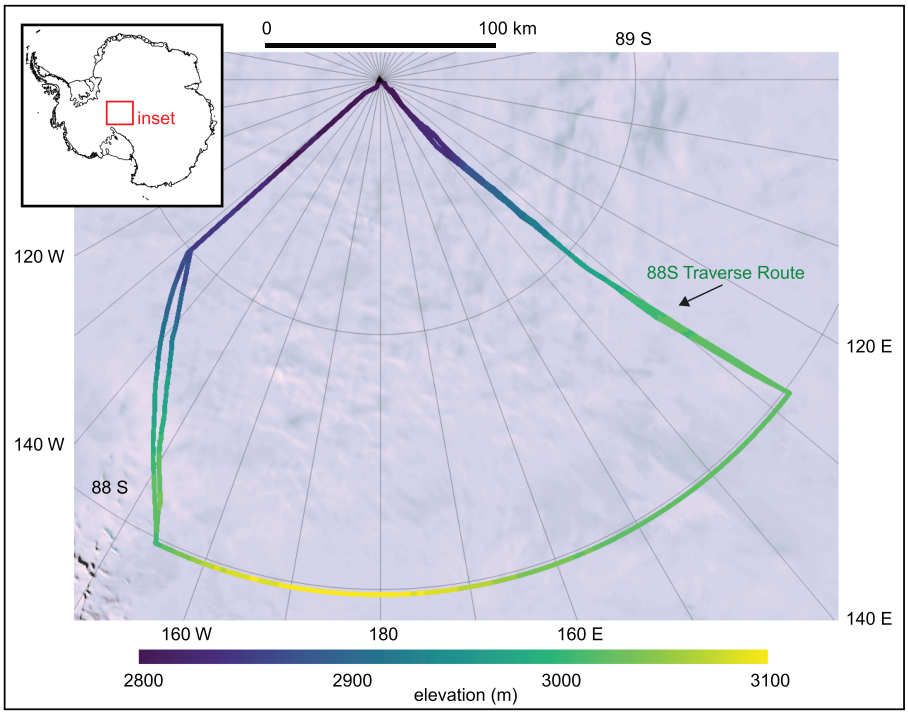


Figure 1. The 88S Traverse map. Color coding is WGS84 height. Background is the Landsat Image of Antarctica (Bindschadler et al., 2008).

3 km across track, to provide greater data density. It takes 91 days to sample all 1,387 unique RGTs or to complete one full orbital cycle.

ICESat-2 has been collecting data since 14 October 2018 and has a suite of data products, including a low-level global product and six higher-level products associated with the various geophysical surface types. ATLAS transmits at 10 kHz, creating footprints every 0.7 m in the along-track direction. Data products include the Global Geolocated Photon Level 2A data product (ATL03; Neumann et al., 2019), which is a large data set comprising latitude, longitude, and ellipsoidal height for every detected photon event. ATL03 also provides a discrimination between photon events that are likely surface-reflected signal photons and those that are likely background photons. The histogram-based algorithm is conservative in that it accepts false positives (classifying a background photon incorrectly as a signal photon) in order to minimize false negatives (Neumann et al., 2019). Higher-level data products build from ATL03, tuned to specific geophysical surface types. This includes Land Ice Along-Track Height Product (ATL06; Smith et al., 2019). ATL06 aggregates photon geolocation information on 40-m along-track length scales, with postings for 20-m along-track segments.

To assess the accuracy of the photon-based and segment-based heights of ATL03 and ATL06, we compared these products with ground-based Global Navigation Satellite Systems (GNSS) height data from the Antarctic ice sheet. ICESat-2 has an orbital inclination of 92°, which results in data coverage between 88° N and 88°S. ICESat-2 data are most dense where the ICESat-2 ground tracks converge. We have conducted two 750-km kinematic GNSS ground traverses in Antarctica, referred to as the 88S Traverse, with the primary area of interest being along 20% (~300 km) of 88°S, which intersects ~275 ICESat-2 RGTs (Figure 1; Brunt et al., 2019).

The 88S Traverse is ideal for satellite accuracy assessment, as time sequential ICESat-2 RGTs are not geographically sequentially spaced; thus, the temporal sampling of the RGTs that intersect the 88S Traverse does not bias any small segment of the ICESat-2 orbital cycle. Since the RGTs intersected by our traverse span the full orbital cycle, environmental factors, such as cloud cover, that often compromise small-scale satellite assessment efforts are mitigated. To date, we have conducted two traverses. The first traverse (2017–2018) occurred 9 months before the ICESat-2 launch and provided an assessment of airborne lidars that will be

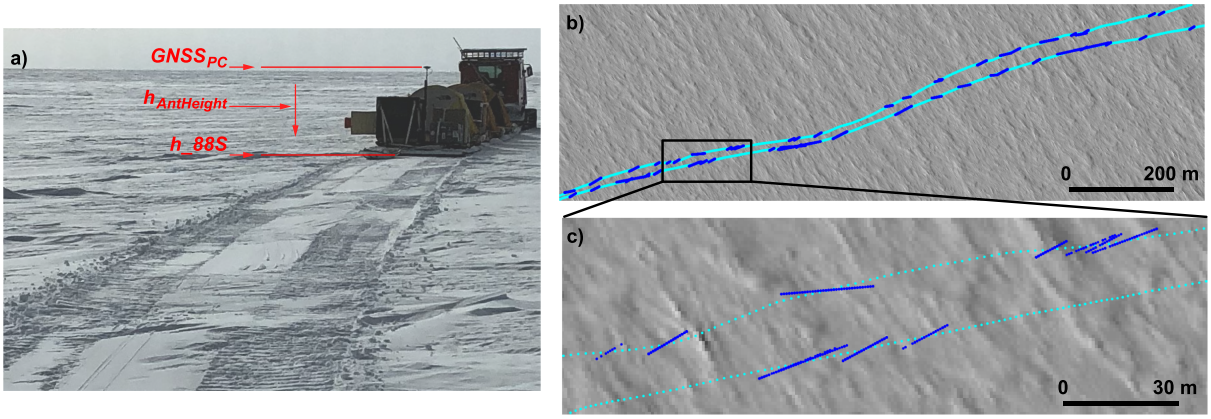


Figure 2. (a) The GNSS antenna configuration on the sleds. $GNSS_{PC}$ is the surveyed position solution of the L1 phase center, and $h_{\mathrm{AntHeight}}$ is the distance between the phase center plane and the snow surface, *h_88S*. (b) Sample ATL03 footprint spacing (blue), where they are within a 2-m search radius of the 88S Traverse GNSS data (cyan). (c) A zoom of the same. WorldView-2 imagery, copyright 2017, DigitalGlobe, Inc.

used for ICESat-2 validation (Brunt et al., 2019). The second traverse (31 December 2018 to 11 January 2019) occurred during early ICESat-2 data collection and is used here for assessing the satellite height data.

Here, we present a comparison between the ICESat-2 ATL03 and ATL06 surface heights and the ground-based GNSS surface heights from the 2018–2019 88S Traverse, providing a first assessment of ICESat-2 performance over ice sheet interiors.

2. Data and Methods

2.1. ICESat-2 Data

We obtained the ATLAS/ICESat-2 L2A Global Geolocated Photon Data (ATL03; Neumann et al., 2019) that are publicly available through the National Snow and Ice Data Center. We assessed Release 001 data collected between 14 October 2018 and 30 April 2019. Similarly, we obtained the ATLAS/ICESat-2 L3A Land Ice Height data (ATL06; Smith et al., 2019), Release 001, through the National Snow and Ice Data Center, for data collected during the same time period. The heights on both ATL03 and ATL06 are given in the ITRF2014 reference frame, and the geographic coordinates are referenced to the WGS84 ellipsoid (Neumann et al., 2019).

ATL03 and ATL06 data are organized by individual ground track. Every ~9 months the orientation of ICESat-2 is rotated 180° to maximize illumination of the solar panels and to keep the spacecraft radiators pointed away from the Sun. Since each beam has a unique path through the instrument, our assessment accounts for the spacecraft reorientation on 28 December 2018 by referring our analysis to the performance of the instrument spots (1 through 6), rather than the ground tracks (GT1L, GT1R, GT2L, GT2R, GT3L, and GT3R).

For each of the six ground tracks, we extracted individual photon heights (*h_ph*), latitudes (*lat_ph*), longitudes (*lon_ph*), a time parameter (*delta_time*), and a surface signal confidence metric (*signal_conf_ph*). Similarly, for each of the ATL06 ground tracks, we extracted surface heights (*h_li*), latitudes (*latitude*), longitudes (*longitude*), a time parameter (*delta_time*), and a surface signal confidence metric (*atl06_quality_summary*). The ATL03 and ATL06 data were subsetted to data near the ground-based GNSS data. We then filtered ATL03 data set by selecting photons of high, medium, and low signal confidence, using the *signal_conf_ph* parameter (Neumann et al., 2019). Similarly, we selected ATL06 data with an overall *atl06_quality_summary* value of 0 (Smith et al., 2019).

2.2. The 2018–2019 88S Traverse GNSS Data

The two 88S Traverses have been conducted using two PistenBully tracked vehicles, provided by the U.S. Antarctic Program. Each PistenBully towed a ~2.5-m-wide and ~20-m-long sled with no runners, made of a single sheet of high molecular weight plastic, which rode smoothly over the ice surface (Figure 2a). The route is generally quite flat, with the overall elevation varying by about 100 m over 300 km (Figure 1).

However, the steady wind creates fields of sastrugi, making the surface rough over shorter (meters to tens of meters) length scales.

The 2018–2019 88S Traverse kinematic GNSS data were collected using continuously operating Septentrio PolaRx5 receivers and PolaNt-x MF antennas, which were provided by the University Navstar Consortium. The antennas were deployed on the smooth-riding rear-center of each sled (Figure 2a). Thus, the effects of both the vehicle tracks and surface roughness were dampened. This change was made based on 2017–2018 traverse experience (Brunt et al., 2019). The antennas were each mounted on fixed staffs attached to large and rigid wooden cargo boxes.

On a typical day, we surveyed for ~7 hr at a speed of ~2 m/s, making periodic stops (approximately four per day). We used GNSS sampling rates of 2 Hz and ran the units continuously except for infrequent system reboots (less than one per day) and short periods for data downloading. GNSS B had a minor amount of data loss (3.5 hr, 8 January 2019) due to a loose wire connection. Given the vehicle velocity and the sampling rate, the GNSS data set has nonuniform spacing, with a characteristic sampling scale of 1 m (Figures 2b and 2c).

GNSS postprocessing methods were based on our assessments of airborne lidar (Brunt et al., 2017, 2019). The 88S Traverse GNSS data were processed using Precise Point Positioning, as implemented in the commercial software package Inertial Explorer (version 8.60). We limited our analysis to geodetic data from the Global Positioning System constellation based on postprocessing difficulties in Inertial Explorer when adding GLObal NAvigation Satellite System data. We processed the data to the L1 antenna phase centers and used a satellite elevation mask of 7.5° to reduce errors associated with GNSS multipath. Inertial Explorer provides a sigma metric for assessing vertical accuracy; a vertical sigma of more than 13 cm was filtered as suspect data. Like the ICESat-2 data, the processed GNSS surface heights are given in the ITRF14 reference frame and the geographic coordinates are referenced to the WGS84 ellipsoid.

The antenna heights for the 88S Traverse were measured using a survey rod from the plane that contained the phase center (as indicated on the antenna) to the base of the sleds, that is, the snow surface (Figure 2a). These measurements were made at the beginning and end of the traverse (and once during the traverse); they were found to be consistent and nearly identical (2.06 m). Thus, to reduce the 88S Traverse GNSS phase center solutions to the height of the snow surface, we simply subtracted the antenna heights. Comparisons were then made between the GNSS data, corrected to the snow surface, and the filtered ICESat-2 data.

2.3. ICESat-2 and 88S Traverse Height Comparisons

We compared the filtered subset of ATL03 surface heights with the processed 2018–2019 88S Traverse GNSS surface heights at their points of intersection. We identified the approximate intersection between ATL03 data and the 10-point smoothed GNSS data using determinants. We then subsetted each data set to ~500 m around the resulting intersection point. We removed from analysis intersections of fewer than 50 signal photons.

Once subsets of a given ATL03 ground track and the GNSS data had been quality-filtered around the intersections, we implemented a "nearest-neighbor" method to assess the satellite height bias. For every signal photon in the ATL03 subset, we found the nearest GNSS data point and calculated the ATL03-GNSS height difference. We limited this height comparison to where the horizontal distance between the signal photon and the nearest GNSS data point was less than 2 m (Figures 2b and 2c). Finally, each intersection had to have at least 30 ATL03-GNSS height comparisons that met the 2-m distance criteria. The bias for an ATL03-GNSS intersection is taken to be the median of these height differences and the surface measurement precision is taken to be the 1σ standard deviation.

Similar methods were implemented for ATL06 segmented surface heights and GNSS height comparisons, with some minor differences. ATL06 segment heights are calculated by aggregating 40 m of along-track photon data, with geolocation information posted regularly every 20 m. Thus, ATL06 is a smaller and smoother data set than ATL03. We searched for all GNSS data that were within a 20 m radial distance from each ATL06 segment-center coordinate. We restricted height comparisons to ATL06 postings that contained at least 30 GNSS height postings within the 20-m search radius. We then calculated the height difference between the ATL06 segment height and the median GNSS height data within the 20-m search radius. The bias for ATL06 is taken to be the median of the residuals at each ATL06 posting, across the entire intersection and the surface measurement precision is taken to be the 1σ standard deviation.

Table 1
ATL03 and ATL06 Surface Bias and Precision Relative to 88S Traverse Data

ATLAS spot	ATL03 bias ± precision (cm)	ATL06 bias ± precision (cm)
1	−0.8 ± 13.1 (N = 659)	−2.8 ± 8.9 (N = 661)
2	+2.0 ± 9.4 (N = 551)	−1.5 ± 8.8 (N = 645)
3	+4.5 ± 8.9 (N = 1,019)	+1.7 ± 7.7 (N = 1,018)
4	+3.6 ± 8.4 (N = 927)	+0.6 ± 7.9 (N = 1,009)
5	+5.1 ± 10.3 (N = 865)	+2.3 ± 7.6 (N = 863)
6	+6.1 ± 10.9 (N = 742)	+2.7 ± 8.1 (N = 805)

Note. ATL03 analysis based on high, medium, and low confidence photons. N represents the total number of ICESat-2-GNSS intersections assessed. ATLAS = Advanced Topographic Laser Altimeter System.

Release 001 of ICESat-2 data still contains blunders, for example background noise that has erroneously been identified as surface signal. We limit the effect of blunders on our overall statistics by removing ICESat-2 data comparisons with height differences larger than 2 m.

3. Results

To assess the quality of the 2018–2019 88S Traverse GNSS height data, we compare of the data sets from each vehicle using a nearest-neighbor method, limiting the search to a 1-m radius. The median residual and the 1σ standard deviation between the GNSS data sets was 0.2 ± 6.3 cm (n = 24,434). If we assume that the errors in the GNSS data sets that contributed to these differences were independent, then the error in a single measurement would be 4.5 cm. These results are similar to those of Brunt et al. (2019), who found a GNSS median residual of 1.1 ± 4.1 cm (n = 26,442) for the 2017–2018 88S Traverse data.

When assessing ICESat-2 surface heights, we consider the 2018–2019 88S Traverse GNSS data to be truth. However, like Brunt et al. (2017, 2019), we acknowledge that there are almost certainly errors within these data, such as formal GNSS errors, Precise Point Positioning methodology limitations (Bisnath & Gao, 2009), and errors associated with the atmosphere (Bar-Sever et al., 1998). The separation in space (< 500 m) and time (<15 min) between the survey vehicles during the 2018–2019 traverse was quite small, and we acknowledge that these results do not consider correlated errors such as those associated with the atmosphere. To assess the magnitude of such errors, we surveyed a ~10 km flat segment near the start of the traverse twice, separated by 13 days. This flat segment is part of the South Pole Traverse, along which heavy tracked vehicles towing heavy sleds with equipment and fuel repeatedly pass, flattening out the sastrugi to produce a relatively smooth and compacted surface. We compared data collected along the South Pole Traverse from the beginning (28 December 2018) and end (10 January 2019) of our 88S Traverse. We merged the GNSS data sets associated with both vehicles and then compared the data from the two different time periods. The difference between the early and late GNSS data sets was 3.9 ± 4.6 cm (n = 12,444). This is the difference between two distinct realizations (separated in time) of the systematic error in the GNSS measurements; thus, our best estimate of the systematic error in ~10 km of GNSS data is 3.3 cm. This value is not a precise assessment of the systematic error because it is based on only one difference. However, it suggests that these errors are on the scale of a few centimeters. Based on this we take the uncertainty in any single measurement to be the quadratic sum of the 4.5-cm error estimated from the spread between the GNSS data sets and this 3.3-cm uncertainty, or 5.6 cm.

We also compared the 2018–2019 and 2017–2018 88S Traverse data sets; the median residual between these data sets was 5.7 ± 12.5 cm (n = 40,903). This precision is worse than the 6.3 cm precision reported for the 2018–2019 88S Traverse, which may be due in part to the changing sastrugi environment between the two field seasons, and in part due to the different atmospheric conditions or accumulation between the two seasons. A similar comparison along the smooth surface of the South Pole Traverse yielded a median residual between these data sets of 1.2 ± 9.6 cm (n = 12,462), suggesting that height differences due to sastrugi play a significant role (~40 % of the variance) in the errors in the rougher areas.

Table 1 presents the comparison of ATL03 and ATL06 surface heights and 88S Traverse GNSS heights. Positive bias values in Table 1 indicate that the ICESat-2 surface is above the GNSS surface. Rejection of ATL03-GNSS differences with greater than 2 m, which we believe are associated with blunders, reduced the data set by 1.2%. Similarly, rejection of ATL06-GNSS differences greater than 2 m resulted in a 0.9% reduction. Surface measurement precision includes ATLAS instrument precision, the impact of geolocation errors of ICESat-2, and geophysical properties that compromise the surface height measurement, such as the atmosphere and surface slope (Brunt et al., 2017, 2019).

4. Discussion

From Table 1, ICESat-2 biases and surface measurement precisions are generally comparable between the spots. These comparisons were restricted to the flat Antarctic ice sheet interior, which provides a strong

Table 2
Unbuffered and Buffered ATL03 Surface Bias and Precision Relative to the 88S Traverse Data

ATLAS spot	ATL03 bias ± precision (cm)	ATL03 bias ± precision (cm; with buffer)	Bias difference (cm)	ATL06*fpb_med_corr* + *tx_med_corr* (cm)
1	−0.8 ± 13.1	−0.7 ± 12.7	−0.1	1.16
2	+2.0 ± 9.4	+0.8 ± 9.6	1.2	1.1
3	+4.5 ± 8.9	+3.4 ± 9.3	1.1	1.2
4	+3.6 ± 8.4	+2.6 ± 8.9	1.0	0.7
5	+5.1 ± 10.3	+3.9 ± 11.0	1.2	0.5
6	+6.1 ± 10.9	+4.6 ± 11.0	1.5	0.4

Note. Column 4 is the difference between these two analyses. Column 5 is the summation of ATL06 "first-photon-bias median" and "pulse-truncation median" corrections. ATLAS = Advanced Topographic Laser Altimeter System.

lidar surface signal return and where the effects of surface slope are minimal. This environment allows us to evaluate ICESat-2 by aggregating large numbers of measurements over a relatively small area, with consistent measurement geometry. Thus, the results presented here are an evaluation of the ICESat-2 data quality over relatively homogenous and low-slope conditions. Differences between ICESat-2 and GNSS heights are due to a combination in the errors in the two data sets, but because the RMS differences and biases are significantly larger than the errors we estimate for the GNSS heights alone (with around 2–4 times the variance), we treat these differences as if they are due mostly to ICESat-2 errors.

Table 1 indicates that ATL06 biases cluster more tightly around 0 than the ATL03 biases, which are generally positive, suggesting that the ATL03 surface is higher than the ATL06 surface. Differences in the algorithms suggest that the ATL03 method is likely truncating the lower part of the surface signal (Neumann et al., 2019; Smith et al., 2019). The ATL03 algorithm returns photon classifications for high, medium, and low confidence surface returns; it also classifies a band of photons around that surface as the "buffer" to ensure that all surface signal photons are provided to upper-level data product algorithms. To confirm that we were capturing the full, untruncated ATLAS surface-return signal, we reassessed the ATL03 surface by including the buffer photons. For the land-ice data product, that buffer is 20 m (Neumann et al., 2019).

Table 2 presents results using the same methodology described in section 3 but including ATL03 buffer photons. Except for ATLAS Spot 1, inclusion of the buffer photons results in a bias approximately 1 cm lower than the biases presented in Table 1. This shifts the ATL03 surface down, toward the ATL06 surface and toward the 88S Traverse GNSS surface. We note that including the buffer has an expected impact on the surface measurement precision; a wider cloud of photons around the surface identified using high, medium, and low confidence signal photons leads to a slight increase in the 1σ standard deviation, again except for Spot 1.

We assume that the mean 1.0 cm differences between the buffered and unbuffered analyses (Table 2) are associated with (1) a detector sensitivity to the leading photons of the reflected distribution (i.e., a first-photon bias; Smith et al., 2019) and (2) the truncation of the reflected pulse during data postprocessing due to both the length of the transmit pulse and any effects of green light penetration into the snow (Gardner & Sharp, 2010). In addition to buffering the signal around the surface, ATL06 makes corrections for these biases and posts these two corrections on the data product: (1) the first-photon-bias median correction (*fpb_med_corr*) and (2) the pulse-truncation median correction (*tx_med_corr*; Smith et al., 2019). Along the 88S Traverse the first-photon-bias correction median value, across all spots, was 2.1 cm, while the pulse-truncation median correction was −1.1 cm, the sum of which (0.9 cm) is comparable to the 1.0-cm estimate of the similar geophysical phenomenon based on the ATL03 analysis. Thus, the corrections developed for the ATL06 product explain the differences between the ATL06 and the unbuffered ATL03 heights and provides a more faithful representation of the surface as measured by GNSS.

The ATL03 and ATL06 biases based on the 88S Traverse data set almost certainly contain a combination of both uncorrelated and correlated errors. These results capture the biases of all spots, for the entire mission through the end of April 2019. However, since this method is effectively a crossover technique, these results do not distinguish between errors associated with a single orbit (such as radial orbit error or errors in our atmospheric range delay correction) and errors that are uncorrelated at short spatial scales (such as those

driven by sampling of the photon distribution or by surface roughness); determining orbit-related error would require the assessment of longer length scales of along-track data, ideally from many different ICESat-2 orbits, to understand the distribution of these error terms.

5. Conclusions

The 88S Traverse provides an excellent assessment data set, given the internal consistency of the GNSS data. Because of the large number of RGTs intersected by the 88S Traverse, this data set also offers a large statistical population and samples many orbital cycles, mitigating the impact of bad weather. Surveying sections of the South Pole Traverse twice, with a large time separation, allowed assessment of the magnitudes of correlated errors. Finally, the 88S Traverse surface is flat over long (tens to hundreds of kilometers) length scales, but is relatively rough, due to sastrugi, on shorter (meters to tens of meters) length scales. Sastrugi migrate from season to season (Gow, 1965), which has an impact on the repeatability of height comparisons; thus, it is important to minimize the gap in time between the data sets being compared. Based on results presented here, over the ice sheet interior, we conclude that ATL03 is currently accurate to better than 5 cm with better than 13 cm of surface measurement precision, while ATL06 is currently accurate to better than 3 cm with better than 9 cm of surface measurement precision.

Acknowledgments

Funding was provided by the NASA ICESat-2 Project Science Office. We thank the ICESat-2 instrument, ground systems, and data product teams. We thank Adam Greeley, Matt Means, Chris Simmons, Chad Seay, and Forrest McCarthy for 88S Traverse support. We thank the National Science Foundation (NSF) Office of Polar Programs for logistical support of the 88S Traverse. We thank NSIDC for ICESat-2 data distribution. We thank the numerous personnel with the U.S. Antarctic Program for their dedication to Polar research. Finally, we thank our Editor (Mathieu Morlighem), Jack Kohler, and one anonymous reviewer for constructive comments that contributed to this manuscript. ICESat-2 data are available via NSIDC (https://nsidc.org/data/icesat-2); 88S Traverse GNSS data are available on the ICESat-2 website (https://icesat-2.gsfc.nasa.gov). WorldView-2 imagery is available to NSF- and NASA-funded researchers via the Polar Geospatial Center at the University of Minnesota, supported by Grant ANT-1043681 from the NSF.

References

Bar-Sever, Y., Kroger, P., & Borjesson, J. (1998). Estimating horizontal gradients of tropospheric path delay with a single GPS receiver. *Journal of Geophysical Research*, *103*(B3), 5019–5035. https://doi.org/10.1029/97JB03534

Bindschadler, R., Vornberger, P., Fleming, A., Fox, A., Mullins, J., Binnie, D., et al. (2008). The Landsat image mosaic of Antarctica. *Remote Sensing of Environment*, *112*(12), 4214–4226. https://doi.org/10.1016/j.rse.2008.07.006

Bisnath, S., & Gao, Y. (2009). Current state of precise point positioning and future prospects and limitations. In *Observing our changing Earth*, (pp. 615–623). Berlin, Heidelberg: Springer.

Brunt, K., Hawley, R., Lutz, E., Studinger, M., Sonntag, J., Hofton, M., et al. (2017). Assessment of NASA airborne laser altimetry data using ground-based GPS data near Summit Station, Greenland. *The Cryosphere*, *11*(2), 681–692. https://doi.org/10.5194/tc-11-681-2017

Brunt, K., Neumann, T., & Larsen, C. (2019). Assessment of altimetry using ground-based GPS data from the 88S Traverse, Antarctica, in support of ICESat-2. *The Cryosphere*, *13*(2), 570–590. https://doi.org/10.5194/tc-13-579-2019

Gardner, A., & Sharp, M. (2010). A review of snow and ice albedo and the development of a new physically based broadband albedo parameterization. *Journal of Geophysical Research*, *115*, F01009. https://doi.org/10.1029/2009JF001444

Gow, A. (1965). On the accumulation and seasonal stratification of snow at the South Pole. *Journal of Glaciology*, *5*(40), 467–477. https://doi.org/10.3189/S002214300001844X

Markus, T., Neumann, T., Martino, A., Abdalati, W., Brunt, K., Csatho, B., et al. (2017). The Ice, Cloud, and land Elevation Satellite-2 (ICESat-2): Science requirements, concept, and implementation. *Remote Sensing of Environment*, *190*, 260–273. https://doi.org/10.1016/j.rse.2016.12.029

Neumann, T. A., Brenner, A. C., Hancock, D. W., Harbeck, K., Luthcke, S., Robbins, J., Saba, J., & Gibbons, A. (2018). Ice, Cloud, and Land Elevation Satellite-2 project algorithm theoretical basis document for global geolocated photons (ATL03). https://icesat-2.gsfc.nasa.gov/science/data-products.

Neumann, T. A., Martino, A. J., Markus, T., Bae, S., Bock, M. R., Brenner, A. C., et al. (2019). The Ice, Cloud, and Land Elevation Satellite-2 Mission: A global geolocated photon product. *Remote Sensing of Environment*, *233*, 111325. https://doi.org/10.1016/j.rse.2019.111325

Smith, B., Fricker, H. A., Holschuh, N., Gardner, A. S., Adusumilli, S., Brunt, K. M., et al. (2019). Land ice height-retrieval algorithms for NASA's ICESat-2 photon-counting laser altimeter. *Remote Sensing of Environment*, *233*, 111352. https://doi.org/10.1016/j.rse.2019.111352